SEMARAK ILMU PUBLISHING

Journal of Advanced Research in Fluid Mechanics and Thermal Sciences

Journal homepage:
https://semarakilmu.com.my/journals/index.php/fluid_mechanics_thermal_sciences/index
ISSN: 2289-7879

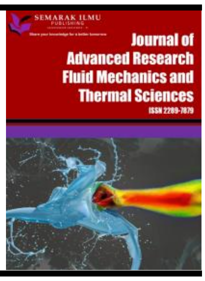

Effects of Dufour and Heat Generation on MHD Casson Fluid Flows Past an Inclined Oscillating Plate with Chemical Reactions and Thermal Radiation in a Rotating Porous Medium

Chinnasamy Manigandan[1], Sathiamoorthy Senthamilselvi[1,*], Sunder Rajan Deepa[2], Periyasamy Selvaraju[3]

[1] Department of Mathematics, Vels Institute of Science, Technology & Advanced Studies, Chennai-600117, Tamil Nadu, India
[2] Department of Mathematics Vel Tech High Tech Dr. Rangarajan Dr. Sakunthala Engineering College, Chennai-600062, Tamilnadu, India
[3] Department of Computer Science and Engineering, Saveetha School of Engineering, SIMATS, Chennai-602105, Tamilnadu, India

ARTICLE INFO

Article history:
Received 8 July 2024
Received in revised form 22 October 2024
Accepted 4 November 2024
Available online 20 November 2024

Keywords:
Dufour; heat generation; MHD; thermal radiation; chemical reaction; rotation

ABSTRACT

An analytical interpretation of unsteady-free convective hydromagnetic boundary layers is given in this work. It illustrates the impacts of Dufour radiation of heat, along with chemical reactions on a Casson fluid flowing by an inclined oscillating plate, a uniform magnetic field, and a rotating porous medium. The governing equations that had been solved by utilising the Laplace transform approach and the outcomes are shown. The numerical values of Casson fluid temperature, concentration, and velocity at the plate are visually represented for a range of relevant parameter values. The non-Newtonian fluid, which moves at a faster speed than the Newtonian fluid, has a Casson fluid parameter, which is examined and explained in this study. Moreover, the temperature trend increases with the Dufour number (Df), heat generation parameter (Q), and the reverse trend for thermal radiation parameter (R), Pradtl number (Pr), Schmidt number (Sc), as well as chemical reaction parameter (K). The concentration falls as the chemical reaction parameter (K) and Schmidt number (Sc) rise. We looked at the sped-up flow after the investigation to get measurable data, making sure to take into account things like Cason fluid parameter, Dofour number, and accumulation. Grashof values also findings speed decreases with increased radiation, chemical reaction, and Schmidth parameter levels. Our significant contribution to this research is an in-depth study of rotation with an inclined oscillating plate, which investigates the relationships between rotational forces, oscillation frequency, plate inclination, magnetic fields, and non-Newtonian features of Casson fluids. This work increases our understanding of how these parameters influence fluid behaviour, heat transfer, and mass transfer by offering a complete analytical framework that can be applied to a wide range of practical problems in fluids.In this research, my main contribution is rotation with an inclined oscillating plate.

[*] *Corresponding author.*
E-mail address: msselvi2305@gmail.com

https://doi.org/10.37934/arfmts.124.1.111127

1. Introduction

Magnetohydrodynamic flows are used in many fields, such as geophysics, electrical power generation, and magnetohydrodynamics. This is why experimental and theoretical studies of them are so important in engineering and technology. There are numerous applications in both science and practice for the transfer of heat from various geometries that have been embedded in porous media. These consist of nuclear reactor cooling, packed-bed catalytic reactors, enhanced oil recovery, geothermal reservoirs, porous solid drying, thermal insulation, and subterranean energy transfer. Numerical simulations of linked radiation and convection processes are currently the focus of much research in radiative heat transfer. Because of its numerous technological applications, convective transfer of heat in the porous medium has received a lot of attention lately. For example, Soundalgekar *et al.,*'s study [1] evaluated the effects of MHD on a vertical infinite plate that underwent temperature fluctuations and transverse magnetic field effects. Chamkha *et al.,* [2] examined the infinite vertical plate radiative free convection flow through a visually thin grey gas. The effects of radiation as well as chemical reactions on the MHD Casson fluid's flow past a vertical plate that moves back and forth in porous medium had been assessed by Kataria and Patel [3]. Vijayaragavan *et al.,* [4] conducted a study to find a theoretical solution for the heat along with mass transfer problem in MHD Casson fluid flow past a sloped porous plate during Dufour and with also chemical reactions. Kavitha *et al.,* [5] reported that they investigated the impacts of uniform temperature along with the mass diffusion on a parabolic flow through a rotating isothermal plate during a chemical reaction. An MHD parabolic flow that travelled through an isothermal plate that was rotating and accelerating has also been assessed by Selvaraj *et al.,* [6]. Naadakumar *et al.,* [7] looked into the Soret and MHD effects of parabolic flow passing by a rapidly moving vertical plate. The plate was also rotating while chemical reactions and thermal radiation were going on. Selvaraj and Jothi [8] looked into how the heat source affected MHD and the radiation-absorbing fluid moving across a plate that was getting higher and higher and had a porous medium around it. According to Lakshmikaanth *et al.,* [9] when radiation (R) goes up, the temperature goes down, but when heat source (Q) goes up, the temperature goes up as well. Maran *et al.,* [10] led a group of researchers to investigate the transfer of mass and heat across a vertical plate during a chemical process or thermal diffusion. MHD did not govern convection flow. Aruna *et al.,* [11] looked into the Hall as well as magnetic effects on a stream travelling past a vertical plate at a parabolically high speed in a different study. The heat was fluctuating, but the mass was dispersing uniformly as thermal radiation. When the flow was not steady, Radha *et al.,* [12] examined the impacts of magnetohydrodynamics on Casson fluid flow past a parabolic accelerated vertical plate having thermal diffusion. The free convection effects on the vertical plate magnetohydrodynamic flow moving during a chemical reaction were examined by Muthucumaraswamy and Ganesan [13] and Muthucumaraswamy *et al.,* [14]. Heat, along with transfer, effects of Hall and rotational phenomena, were studied in relation to magnetohydrodynamic flow over a vertically orientated plate experiencing exponential acceleration. Hetnarski [15,16] demonstrates how to use an algorithm to find the formulas for inverse Laplace transforms. The issue of the non-steady MHD flow Dufour effect passing through a vertical plate in porous medium by rising temperature has been examined and resolved by Sarma and Ahmed [17]. The radiation and also the heat effects on MHD and parabolic motion in Casson fluids flowing by a spinning porous medium on a vertical plate have been examined by Prakash and Selvaraj [18]. In a study by Reddy *et al.,* [19] the effects of thermodynamics, spinning, and diffusion were investigated using computers to analyse the flow of a heat-generating MHD Casson fluid past a moving porous plate. The Soret and Dufour effects on MHD Casson Fluid Over a Vertical Plate in the existence of radiation along with the chemical reaction have been recognised and corrected by Reddy and

Janardhan [20]. The MHD nanofluid flow past a tilted plate and implications of Soret and Dufour were covered by Palani and Arutchelvi [21]. The effects of magnetohydrodynamics (MHD) on a vertical plate fired off infinitely and quickly while temperature changes in the horizontal magnetic field's existence were investigated in the studies by Kumar and Vempati [22] and Vempati and Laxmi-Narayana-Gari [23]. Muthucumaraswamy and Radhakrishnan [24] and Muthucumaraswamy *et al.,* [25] examined how chemical reactions affect flow past a vertical plate that is moving quickly, has mass diffusion, and varies in temperature in the magnetic field's existence. The effects of heat production and cross-diffusion on the mixed convective MHD flow of Casson fluid by a porous medium having non-linear thermal radiation were investigated by Patel [26]. In coumarin 3-(1-methly-2-imiadazolythio)-1-oxoethly, Dhanalakshmi *et al.,*'s study [27] covered the molecules in addition to bond stability, kinetic stability, energy-related factors, and Gc-MS. Karthikeyan *et al.,*'s [28] and Karthikeyan and Selvaraj [29] examined the rotational effects of parabolic flow past an isothermal vertical plate using MHD. The Soret and Dufour effect on unsteady MHD convection flow over an infinite vertical porous plate was studied by Gayathri *et al.,* [30]. In contrast to a rotating fluid with constant temperature along with the diffusion of mass, we examined the Dufour effects of an MHD Casson fluid flowing past an inclined oscillating plate, which accelerates exponentially in this paper. Kumar *et al.,* [31,32] studied the Soret and Dufour's Influence on Unsteady MHD Oscillatory Casson Fluid Flow via an Inclined Vertical Porous Plate in the Presence of Chemical Reaction. also studied the value of heat and mass transfer in MHD flow over a vertical porous plate with chemical reaction and heat generation. Lakshmikaanth *et al.,* [33,34] investigate the parabolic flow over an infinite vertical plate with rotation, chemical reaction, and radiation in the presence of the Hall Effect, Dufour Effect, and heat source in a porous medium. also find out Hall and heat source effects of flow state on a vertically accelerating plate in an isothermal environment, including chemical reactions, rotation, radiation, and the Dufour effect. Rafique *et al.,* [35,36] solved the efficiency of the hall effect under different viscosity and slip circumstances on rotating hybrid nanofluid flow over a nonlinear radiative surface and solved the effects of heat radiation on unsteady bidirectional rotating stagnation point flow of nanofluid with aggregation of nanoparticles and variable viscosity. Adnan *et al.,* [37] examined the heat feature of a radiative convective ternary nanofluid in the presence of a heat-generating source and an induced magnetic field. Khan *et al.,* [38] investigated and solved the mass and heat transfer in the Riga plate's unstable stagnation point flow with impacts from thermal radiation and binary chemical reactions. Ganie *et al.,* [39] find out the solution of the Yamada-Ota model for unstable non-axisymmetric MHD Homann stagnation point flow of CNT-suspended nanofluid over convective surfaces with radiation. This research looks at and clarifies the comparison to Newtonian fluids, Casson fluids tend to show higher velocities in specific situations, such as when a lower yield stress is present or when the applied force above the yield threshold. In contrast to Newtonian fluids, which preserve a linear relationship between stress and strain rate, this permits the non-Newtonian Casson fluid to move more freely in specific domains.

2. Mathematical Formulation

Imagine an unstable free hydromagnetic natural convective flow that moves mass and heat through an infinitely angled oscillating plate built in a rotating system where the fluid's Dufour effect and the Hall current with rotation are both taken into account. The fluid has optical thickening, electrical conductivity, viscosity, and incompressibility. The coordinate model which has been chosen in a way where $x'-$ axis is upward to the plate and $y'-$ The axis is perpendicular to plate. The fluid and plate which has been revolve along $x'-$ axis in with respect to the standardized angular velocity Ω. The fluid and plate which are initially rest at period along $t' \leq 0$ and have been then held at

T'uniform temp . Also, on plate surface, and at the any point which is inside the fluid, concentration of the species at C'_∞ should be conserved uniformly. At the time $t' \geq 0$, plate statistics moving to their own planes at velocity $of\ u' = u_0 coswt$. Where $B_0\ is\ the$ uniform transverse magnetic field which has been applied in a direction which is parallel to $y' -$ axis. The temperature of flow along with the concentration of species on surface of plate are upturned to a uniform temp. of about T'_w and uniform species concentration C'_w and therefore maintained. The problem geometry has been represented in Figure 1. Under these conditions, the flow characteristics solely depend on y' and t Plate temp is declined or rised to $\mathrm{T}'_\infty + (\mathrm{T}'_w - \mathrm{T}'_\infty)\frac{{u_0}^2\bar{t}}{v}$ at $\bar{t} \geq 0$ and concentration of plate is elevated or reduced to $\mathrm{C}'_\infty + (\mathrm{C}'_w - \mathrm{C}'_\infty)\frac{{u_0}^2\bar{t}}{v}$ at $\bar{t} \geq 0$. The rheological state equation for Casson fluid Cauchy stress tensor is represented as follows:

$$\tau_{ij=}\begin{Bmatrix} 2e_{ij}\left(\mu_B + \frac{py}{\sqrt{2\pi}}\right)\ \pi > \pi_c \\ 2e_{ij}\left(\mu_B + \frac{py}{\sqrt{2\pi_c}}\right)\ \pi < \pi_c \end{Bmatrix} \tag{1}$$

The following equations govern the transient flow, taking into account these assumptions

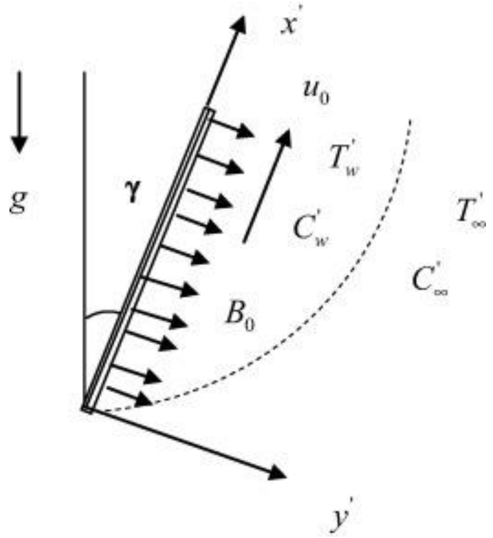

Fig. 1. Physical of model of problem

$$\frac{\partial \mathrm{u}'}{\partial \mathrm{t}'} - 2\Omega'\mathrm{v}' = \vartheta\left(1 + \frac{1}{\gamma}\right)\frac{\partial^2 \mathrm{u}'}{\partial {\mathrm{y}'}^2} + \mathrm{g}\beta_{\mathrm{T}'}(\mathrm{T}' - \mathrm{T}'_\infty)\cos\alpha + \mathrm{g}\beta_{\mathrm{C}'}(\mathrm{C}' - \mathrm{C}'_\infty)\cos\alpha - \frac{\sigma B_0^2\mu^2(u' + h_1 v')}{\rho(1 + h_1^2)} - \frac{\vartheta \mathrm{u}'}{k_1'} \tag{2}$$

$$\frac{\partial \mathrm{v}'}{\partial \mathrm{t}'} + 2\Omega'\mathrm{u}' = \vartheta\frac{\partial^2 \mathrm{v}'}{\partial {\mathrm{y}'}^2} - \frac{\sigma B_0^2\mu^2(h_1 u' - v')}{\rho(1 + h_1^2)} - \frac{\vartheta u'}{k_1'} \tag{3}$$

$$\frac{\partial \theta'}{\partial t'} = \frac{k}{\rho C_p}\frac{\partial^2 \theta'}{\partial {y'}^2} - \frac{1}{\rho C_p}\frac{\partial q_r'}{\partial y'} + \frac{Q_0}{\rho C_p}(\mathrm{T}' - \mathrm{T}'_\infty)' + \frac{D_m K_T}{C_S C_p}\frac{\partial^2 C'}{\partial {y'}^2} \tag{4}$$

$$\frac{\partial \mathrm{C}'}{\partial \mathrm{t}'} = \frac{1}{S_c}\frac{\partial^2 \mathrm{C}'}{\partial {\mathrm{y}'}^2} - k'\,(\mathrm{C}' - \mathrm{C}'_\infty) \tag{5}$$

Under the initial and boundary circumstances specified below

$$\left.\begin{array}{c} u' = 0, v' = 0, T' = T'_\infty,\ C' = C'_\infty,\ \text{for all } z' \geq 0, t' \leq 0 \\ u' = u_0 coswt, T' = T'_\infty + (T'_w - T'_\infty)\frac{t'}{t_0}, C' = (C'_w - C'_\infty)\ \frac{t'}{t_0} \\ u' \to 0, T' \to T'_\infty, C' \to C'_\infty \text{ as } z' \to \infty \text{ and } t' \geq 0 \end{array}\right\} \tag{6}$$

Since our Casson fluid is optically thick, we can apply the Rosseland approximation [26]

$$\frac{\partial q_r}{\partial z'} = -4a^*\sigma\left(T'^4_\infty - T'^4\right) \tag{7}$$

It is considered that there are enough slight temperature variations within the flow, such as T'-4. They could be described as a temperature function that is linear. To achieve this, the Taylor series about, T'∞ is expanded, T'4, while higher-order terms are ignored.

$$T'^4 \cong 4T'^3_\infty T' - 3T'^4_\infty \tag{8}$$

Consequent dimensionless aggregate is

$$\left.\begin{array}{c} U = \frac{u'}{U_0}, V = \frac{v'}{U_0}, t = \frac{t'}{t_0}, y = \frac{y'}{U_0 t_0}, \gamma = \frac{\mu_{B\sqrt{2\pi_c}}}{P_y} \\ = \frac{T'-T'_\infty}{T'_w - T'_\infty}, G_r = \frac{g\beta(T'_w - T'_\infty)}{u_0}, C = \frac{C'-C'_\infty}{C'_w - C'_\infty}, G_C = \frac{g\beta(C'-C'_\infty)}{C'_w - C'_\infty}, Q = \frac{Q_0 v^2}{kU_0^2} \\ P_r = \frac{\mu C_p}{k}\ ,\ K\ = \frac{vk_1}{U_0^2},\ S_c = \frac{v}{D},\ M^2 = \frac{\sigma B_0^2}{\rho U_0^2}v, R = \frac{16a^*\sigma T'^3_\infty}{kU_0^2} \end{array}\right\} \tag{9}$$

Substituting values from Eq. (6) and Eq. (7) in Eq. (3) and in Eq. (1) to Eq. (4) and then we will get the non-dimensional equations are

$$\frac{\partial U}{\partial t} = \left(1 + \frac{1}{\gamma}\right)\frac{\partial^2 U}{\partial y^2} + 2\Omega v - \frac{M^2(U+hV)}{(1+h^2)} + Gr\theta(cos\alpha) + GcC(cos\alpha) - \frac{U}{k_1} \tag{10}$$

$$\frac{\partial V}{\partial t} = \left(1 + \frac{1}{\gamma}\right)\frac{\partial^2 V}{\partial y^2} - 2\Omega v + \frac{M^2(hU-V)}{(1+h^2)} - \frac{V}{k_1} \tag{11}$$

$$\frac{\partial \theta}{\partial t} = \frac{1}{P_r}\frac{\partial^2 \theta}{\partial y^2} - R\theta + Q\theta + Df\,\frac{\partial^2 C}{\partial z^2} \tag{12}$$

$$\frac{\partial C}{\partial t} = \frac{1}{S_c}\frac{\partial^2 C}{\partial y^2} - KC \tag{13}$$

To solve Eq. (1) and Eq. (2), use $q' = U + iV$ we get

$$\frac{\partial q'}{\partial t} = G_r\theta cos(\alpha) + G_C C\cos(\alpha) + \left(1 + \frac{1}{\gamma}\right)\frac{\partial^2 q}{\partial y^2} - m^* q' \tag{14}$$

$$\frac{\partial \theta}{\partial t} = \frac{1}{P_r}\frac{\partial^2 \theta}{\partial y^2} - R\theta + Q\theta + Df\,\frac{\partial^2 C}{\partial y^2} \tag{15}$$

$$\frac{\partial C}{\partial t} = \frac{1}{S_c}\frac{\partial^2 C}{\partial y^2} - KC \tag{16}$$

Here $m^* = 2\left[\frac{M^2}{h^2+1} + i\left(\Omega - \frac{M^2 h}{1+h^2}\right)\right] + \frac{1}{k_1}$.

Corresponding initial and boundary conditions are

$$\left.\begin{array}{c} q' = 0, \theta = 0, C = 0 \; for \; all \; y \; and \; t \leq 0 \\ q' = coswt, \theta = 1, C = 1 \; for \; all \; y \; and \; t \leq 0 \\ q' \to 0, \theta \to 0, C \to 0 \; as \; y \to \infty \end{array}\right\} \tag{17}$$

3. Mathematical Solution of the Problem

Eq. (14), Eq. (15), and Eq. (16) contain dimensionless administering conditions and corresponding beginning and limit conditions. These equations can be solved using Laplace transforms. After lLpalace inverse transform, The solutions are obtained using the subsequent procedure.

$$C = \frac{1}{2}\left[e^{-2\eta\sqrt{ScKt}}\, erfc\left(\eta\sqrt{Sc} - \sqrt{Kt}\right) + e^{2\eta\sqrt{ScKt}}\, erfc\left(\eta\sqrt{Sc} + \sqrt{Kt}\right)\right] \tag{18}$$

$$\theta = \theta_1 + \frac{P_r D_f S_c}{(S_c - P_r)}\left(\frac{a+K}{a}\right)[\theta_2 + \theta_3] + \frac{P_r D_f S_c}{(S_c - P_r)}\frac{K}{a}[\theta_5 + \theta_6] \tag{19}$$

Here

$$\theta_1 = \frac{1}{2}\begin{bmatrix} e^{-2\eta\sqrt{P_r(R-Q)t}}\, erfc\left(\eta\sqrt{Pr} - \sqrt{(R-Q)t}\right) \\ +e^{2\eta\sqrt{P_r(R-Q)t}}\, erfc\left(\eta\sqrt{Pr} + \sqrt{(R-Q)t}\right) \end{bmatrix}$$

$$\theta_2 = \frac{e^{at}}{2}\begin{bmatrix} e^{-2\eta\sqrt{P_r(a+R-Q)t}}\, erfc\left(\eta\sqrt{Pr} - \sqrt{(a+R-Q)t}\right) \\ +e^{2\eta\sqrt{P_r(a+R-Q)t}}\, erfc\eta\sqrt{Pr} + \sqrt{(a+R-Q)t} \end{bmatrix}$$

$$\theta_3 = \frac{e^{at}}{2}\begin{bmatrix} e^{-2\eta\sqrt{S_c(a+K)t}}\, erfc\left(\eta\sqrt{S_c} - \sqrt{(a+K)t}\right) \\ +e^{2\eta\sqrt{S_c(a+K)t}}\, erfc\left(\eta\sqrt{S_c} + \sqrt{(a+K)t}\right) \end{bmatrix}$$

$$\theta_4 = \frac{1}{2}\left[e^{-2\eta\sqrt{S_c Kt}}\, erfc\left(\eta\sqrt{S_c} - \sqrt{Kt}\right) + e^{2\eta\sqrt{S_c Kt}}\, erfc\left(\eta\sqrt{S_c} + \sqrt{Kt}\right)\right]$$

$$\theta_5 = \frac{1}{2}\begin{bmatrix} e^{-2\eta\sqrt{P_r(R-Q)t}}\, erfc\left(\eta\sqrt{Pr} - \sqrt{(R-Q)t}\right) \\ +e^{2\eta\sqrt{P_r(R-Q)t}}\, erfc\eta\sqrt{Pr} + \sqrt{(R-Q)t} \end{bmatrix}$$

$$q' = f_1 + f_2 + \frac{Gr(cos\alpha)}{a_1}\left[\begin{array}{l} f_3 - f_4 + \frac{PrDfSc}{Sc-Pr}\left(\frac{k+a}{a}\right)\left\{\frac{1}{a-c_1}(f_5 - f_6 - f_7 + f_8) - \frac{1}{a-d}(f_9 - f_{10} - f_{11} + f_{12})\right\} \\ \quad + \frac{PrDfSc}{Sc-Pr}\left(\frac{k}{a}\right)\left\{\frac{1}{d}(-f_{13} + f_{14} + f_{15} - f_{16}) - \frac{1}{c_1}(-f_{17} + f_{18} + f_{19} - f_{20})\right\} \end{array}\right] + \frac{Gc(cos\alpha)}{a_1 b}\left[f_{21} - f_{22} - f_{23} + f_{24}\right] \quad (20)$$

$$f_{1}= \frac{e^{-iwt}}{4}\left[\begin{array}{l} e^{-2\eta\sqrt{\frac{(m-iw)t}{a_1}}} erfc\left(\frac{\eta}{\sqrt{a_1}} - \sqrt{(m-iw)t}\right) \\ + e^{2\eta\sqrt{\frac{(m-iw)t}{a_1}}} a_1 erfc\left(\frac{\eta}{\sqrt{a_1}} - \sqrt{(m-iw)t}\right) \end{array}\right]$$

$$f_2 = \frac{e^{iwt}}{4}\left[\begin{array}{l} e^{-2\eta\sqrt{\frac{(m+iw)t}{a_1}}} erfc\left(\frac{\eta}{\sqrt{a_1}} - \sqrt{(m+iw)t}\right) \\ + e^{2\eta\sqrt{\frac{(m-iw)t}{a_1}}} erfc\left(\frac{\eta}{\sqrt{a_1}} + \sqrt{(m+iw)t}\right) \end{array}\right]$$

$$f_3 = \frac{e^{c_1 t}}{2}\left[e^{-2\eta\sqrt{\frac{(m+c_1)t}{a_1}}} erfc\left(\eta - \sqrt{\frac{(m+c_1)t}{a_1}}\right) + e^{2\eta\sqrt{\frac{(m+c_1)t}{a_1}}} erfc\left(\eta + \sqrt{\frac{(m+c_1)t}{a_1}}\right)\right]$$

$$f_4 = f_8 = f_{20} = \frac{e^{c_1 t}}{2}\left[\begin{array}{l} e^{-2\eta\sqrt{Pr(R+c_1-Q)t}} erfc\left(\eta\sqrt{Pr} - \sqrt{(R+c_1-Q)t}\right) \\ + e^{2\eta\sqrt{Pr(R+c_1-Q)t}} erfc\left(\eta\sqrt{Pr} + \sqrt{(R+c_1-Q)t}\right) \end{array}\right]$$

$$f_5 = \frac{e^{at}}{2}\left[e^{-2\eta\sqrt{\frac{(m+a)t}{a_1}}} erfc\left(\eta - \sqrt{\frac{(m+a)t}{a_1}}\right) + e^{2\eta\sqrt{\frac{(m+a)t}{a_1}}} erfc\left(\eta + \sqrt{\frac{(m+a)t}{a_1}}\right)\right]$$

$$f_6 = f_{18} = \frac{e^{c_1 t}}{2}\left[e^{-2\eta\sqrt{\frac{(m+c_1)t}{a_1}}} erfc\left(\eta - \sqrt{\frac{(m+c_1)t}{a_1}}\right) + e^{2\eta\sqrt{\frac{(m+c_1)t}{a_1}}} erfc\left(\eta + \sqrt{\frac{(m+c_1)t}{a_1}}\right)\right]$$

$$f_7 = \frac{e^{at}}{2}\left[\begin{array}{l} e^{-2\eta\sqrt{Pr(R+a-Q)t}} erfc\left(\eta\sqrt{Pr} - \sqrt{(R+a-Q)t}\right) \\ + e^{2\eta\sqrt{Pr(R+a-Q)t}} erfc\left(\eta\sqrt{Pr} + \sqrt{(R+a-Q)t}\right) \end{array}\right]$$

$$f_9 = \frac{e^{at}}{2}\left[e^{-2\eta\sqrt{\frac{(m+a)t}{a_1}}} erfc\left(\eta - \sqrt{\frac{(m+a)t}{a_1}}\right) + e^{2\eta\sqrt{\frac{(m+a)t}{a_1}}} erfc\left(\eta + \sqrt{\frac{(m+a)t}{a_1}}\right)\right]$$

$$f_{10} = \frac{e^{dt}}{2}\left[e^{-2\eta\sqrt{\frac{(m+d)t}{a_1}}} erfc\left(\eta - \sqrt{\frac{(m+d)t}{a_1}}\right) + e^{2\eta\sqrt{\frac{(m+d)t}{a_1}}} erfc\left(\eta + \sqrt{\frac{(m+d)t}{a_1}}\right)\right]$$

$$f_{11} = \frac{e^{at}}{2}\left[\begin{array}{l} e^{-2\eta\sqrt{Sc(a+k)t}} erfc\left(\eta\sqrt{Sc} - \sqrt{(a+k)t}\right) \\ + e^{2\eta\sqrt{Sc(a+k)t}} erfc\left(\eta\sqrt{Sc} + \sqrt{(a+k)t}\right) \end{array}\right]$$

$$f_{12}=\frac{e^{dt}}{2}\begin{bmatrix} e^{-2\eta\sqrt{Sc(d+k)t}}erfc\left(\eta\sqrt{Sc}-\sqrt{(d+k)t}\right) \\ +e^{2\eta\sqrt{Sc(d+k)t}}erfc\left(\eta\sqrt{Sc}+\sqrt{(d+k)t}\right)\end{bmatrix}$$

$$f_{13}=\frac{1}{2}\left[e^{-2\eta\sqrt{\frac{mt}{a_1}}}erfc\left(\eta-\sqrt{\frac{mt}{a_1}}\right)+e^{2\eta\sqrt{\frac{mt}{a_1}}}erfc\left(\eta+\sqrt{\frac{mt}{a_1}}\right)\right]$$

$$f_{14}=\frac{e^{dt}}{2}\left[e^{-2\eta\sqrt{\frac{(m+d)t}{a_1}}}erfc\left(\eta-\sqrt{\frac{(m+d)t}{a_1}}\right)+e^{2\eta\sqrt{\frac{(m+d)t}{a_1}}}erfc\left(\eta+\sqrt{\frac{(m+d)t}{a_1}}\right)\right]$$

$$f_{15}=f_{24}=\frac{1}{2}\left[e^{-2\eta\sqrt{Sckt}}erfc\left(\eta\sqrt{Sc}-\sqrt{kt}\right)+e^{2\eta\sqrt{Sckt}}erfc\left(\eta\sqrt{Sc}+\sqrt{kt}\right)\right]$$

$$f_{16}=\frac{e^{dt}}{2}\left[e^{-2\eta\sqrt{Sc(d+k)t}}erfc\left(\eta\sqrt{Sc}-\sqrt{(d+k)t}\right)+e^{2\eta\sqrt{Sc(d+k)t}}erfc\left(\eta\sqrt{Sc}+\sqrt{(d+k)t}\right)\right]$$

$$f_{17}=\frac{1}{2}\left[e^{-2\eta\sqrt{\frac{mt}{a_1}}}erfc\left(\eta-\sqrt{\frac{mt}{a_1}}\right)+e^{2\eta\sqrt{\frac{mt}{a_1}}}erfc\left(\eta+\sqrt{\frac{mt}{a_1}}\right)\right]$$

$$f_{19}=\frac{1}{2}\begin{bmatrix} e^{-2\eta\sqrt{Pr(R-Q)t}}erfc\left(\eta\sqrt{Pr}-\sqrt{(R-Q)t}\right) \\ +e^{2\eta\sqrt{Pr(R-Q)t}}erfc\left(\eta\sqrt{Pr}+\sqrt{(R-Q)t}\right)\end{bmatrix}$$

$$f_{21}=\frac{e^{bt}}{2}\left[e^{-2\eta\sqrt{\frac{(m+b)t}{a_1}}}erfc\left(\eta-\sqrt{\frac{(m+b)t}{a_1}}\right)+e^{2\eta\sqrt{\frac{(m+b)t}{a_1}}}erfc\left(\eta+\sqrt{\frac{(m+b)t}{a_1}}\right)\right]$$

$$f_{22}=\frac{1}{2}\left[e^{-2\eta\sqrt{\frac{mt}{a_1}}}erfc\left(\eta-\sqrt{\frac{mt}{a_1}}\right)+e^{2\eta\sqrt{\frac{mt}{a_1}}}erfc\left(\eta+\sqrt{\frac{mt}{a_1}}\right)\right]$$

$$f_{23}=\frac{e^{bt}}{2}\begin{bmatrix} e^{-2\eta\sqrt{Sc(b+k)t}}erfc\left(\eta\sqrt{Sc}-\sqrt{(b+k)t}\right) \\ +e^{2\eta\sqrt{Sc(b+k)t}}erfc\left(\eta\sqrt{Sc}+\sqrt{(b+k)t}\right)\end{bmatrix}$$

$$erfc(a+ib)=\mathrm{erf}(a)+\frac{\exp(-a^2)}{2a\pi}[1-\cos(2ab)+isin(2ab)]+$$
$$\frac{2\exp(-a^2)}{\pi}\sum_{n=1}^{\infty}\frac{\exp\left(-\frac{\eta^2}{4}\right)}{\eta^2+4a^2}[f_n(a,b)+ig_n(a,b)]+\in(a,b)$$

$f_n=2a-2\,\mathrm{acosh}(nb)\cos(2ab)+nsinh(nb)\sin(2ab)$, and

$$g_n=2\,\mathrm{acosh}(nb)\sin(2ab)+nsinh(nb)\cos(2ab)$$

$$|\epsilon(a,b)|\approx\approx 10^{-16}|\mathrm{erf}(a+ib)|$$

4. Results and Discussions

We will examine some numerical values that illustrate the impact of different non-dimensional flow characteristics on the speed (q'), concentration (C), and temperature (θ) as they are plotted against the boundary layer coordinate (η) in Figure 2 through Figure 20. The aforementioned numerical values comprise the magnetic parameter (M), chemical reaction parameter (K), rotation parameter (R), heat absorption coefficientn (Q), Dufour number (Df), Casson fluid parameter (γ), time t, Schmidt number (Sc), Grashof numbe(Gr) and permeability parameter (k1).

In Figure 2, the concentration (conc) increases with time ttt, particularly for a range of Schmidt numbers Sc=0.1 to 1000. The Schmidt number Sc represents the ratio of momentum diffusivity to mass diffusivity, and for lower Sc diffusion dominates. As time progresses, particles have more time to diffuse, which results in an increase in concentration, especially for lower Schmidt numbers, where mass diffusion is more significant. In Figure 3, the concentration decreases with increasing values of the chemical reaction parameter K. This shows that higher chemical reaction rates lead to a faster depletion of species, reducing the concentration. A strong chemical reaction enhances the consumption of the diffusing species, leading to a decrease in concentration as K increases.

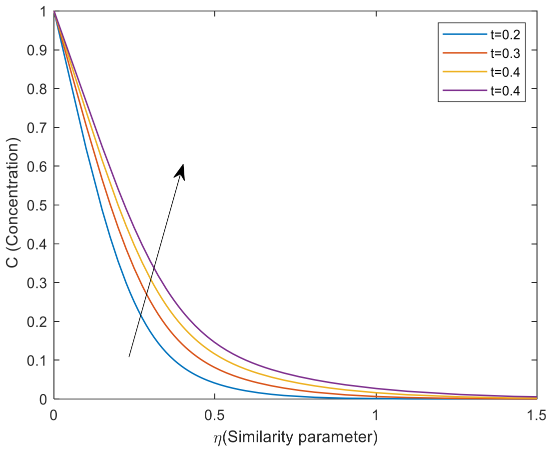

Fig. 2. Concentration curves noted for various values of t and Sc=2.01, K=0.5

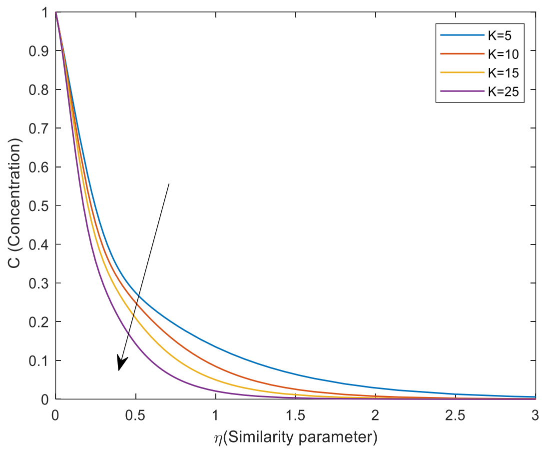

Fig. 3. Concentration curves noted for various values of K and t=0.2, Sc=2.01

Figure 4 illustrates the outcome using different Schmidt numbers. It is possible to see that the divided concentration increases when the Schmidt value is taken to be high. Figure 5 illustrates how the temperature drops as the Pr (Pr= 0.71 for air and Pr=7 for water) values rise. Schmidt number is seen to increase in Figure 6, suggesting an initial capacity of temperature to increase (Range of Schimdt number Range Sc=0.1 to 1000 for liquid). However, the temperature fluctuates after that, indicating a shift in the pattern and a fall in warmth at times. Figure 7 illustrates the profile of temperature showing that the Thermal radiation parameter R goes up, and the temperature goes down.

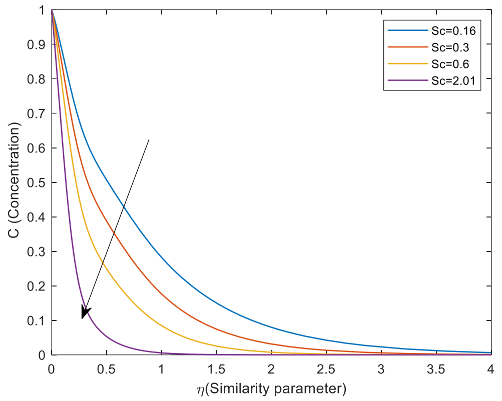

Fig. 4. Concentration profile for various values of Sc and t-0.2, k-10

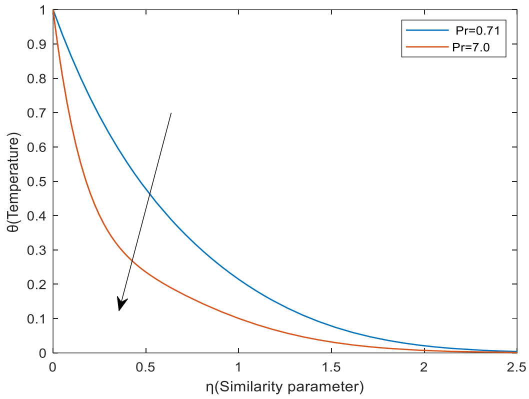

Fig. 5. Temperature Profiles for several values of Pr and Sc=0.6, R=5, Q=1, K=1, Df=1, t=0.2

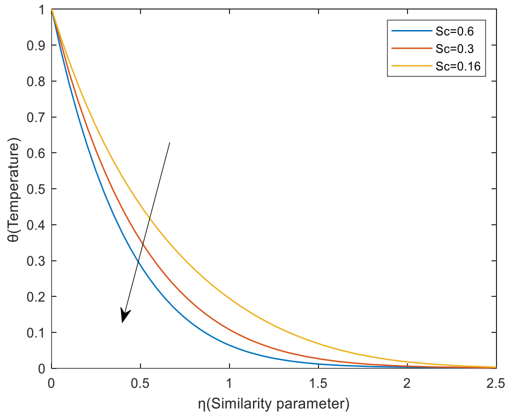

Fig. 6. Temperature profile for multiple of Sc and R=5, Q=1, K=1, Df=1, t=0.2, Pr=0.71

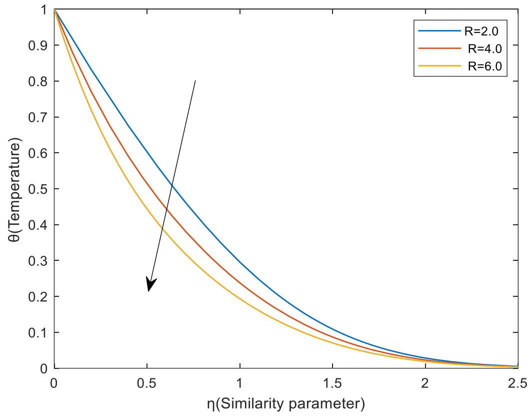

Fig. 7. Temperature Profiles for multiple values of Chemical Reaction K and Pr=0.71, Sc=0.6, Q=1, K=1, Df=1, t=0.2

Figure 8 demonstrates that as the value of temperature falls, the values of chemical reactions K rise. Figure 9 displays the temp behavior for times t = 0.1, 0.2 and 0.3. The fluid's reaction to temp.variations becomes increasingly obvious over time. With time, the temperature rises. We can examine the heat behavior in Figure 10 in greater detail by taking into account the thermal diffusion (Dufour) numbers (Df = 0.1, 1, 2). Generally speaking, an increase in the Dufour parameter indicates a stronger Dufour effect and a greater impact of concentration gradients on the mixture's temperature distribution. As a result, which depends on details along with direction of the Dufour effect, temperatures may rise or fall. The relationship between temperature and the heat generation parameter Q values has been depicted Figure 11.

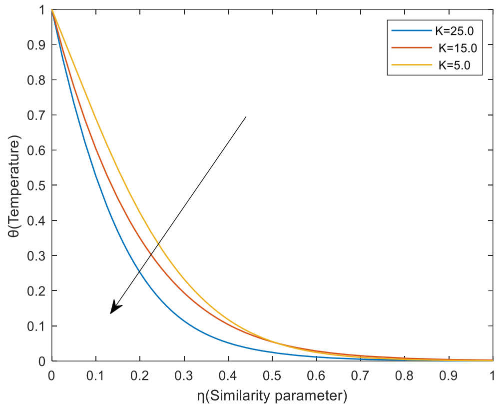

Fig. 8. Temperature profiles of various Chemical Reaction 'K' and Pr=0.71, Sc=0.6, R=2, Q=1, Df=1, t=0.2"

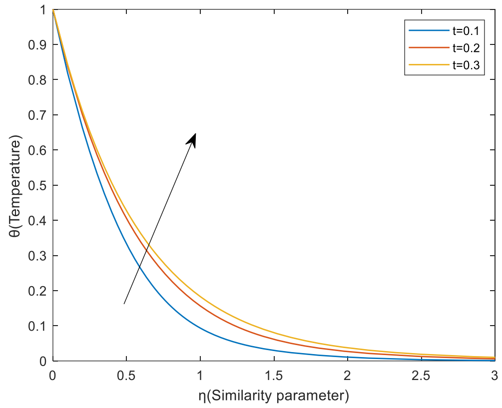

Fig. 9. Temperature Curves for various values of t and Pr=0.7, Sc=0.6, R=6, Q=1, K=5, Df=1

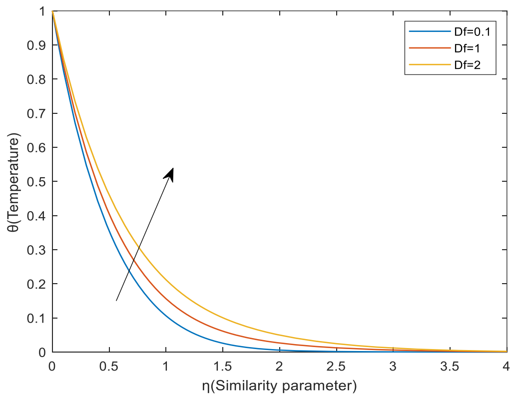

Fig. 10. Temperature profile for various Values of Df and Pr=0.71, Sc=0.6, R=6, Q=0.1, K=5, t=0.2

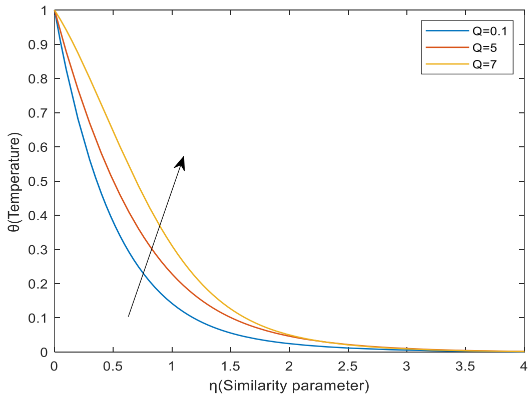

Fig. 11. Temperature profile for various values of Q and Pr=0.71, Sc=0.16, R=6, K=5, Df=1, t=0.2

In Figure 12, It has been found that velocity rises as Prandtl no. values rise. In Figure 13, it was observed that the magnetic field's impact on fluid motion is measured using Hartmann values, which specifically gauge the reduction of velocity variations owing to the Lorentz force of the magnetic field. However, these values do not directly dictate the speed or orientation of the velocity. Figure 14, illustrates the speed for thermal diffusion values (Df = 0.2, 0.3, 0.4), It is clear that when the Dufour no. rises, the fastest speed is attained. Figure 15 displays the plate's velocity contours at many Schmidt values. (0.1, 0.3, and 0.6 for Sc). As speed increases, a plate's Schmidt no. decreases.

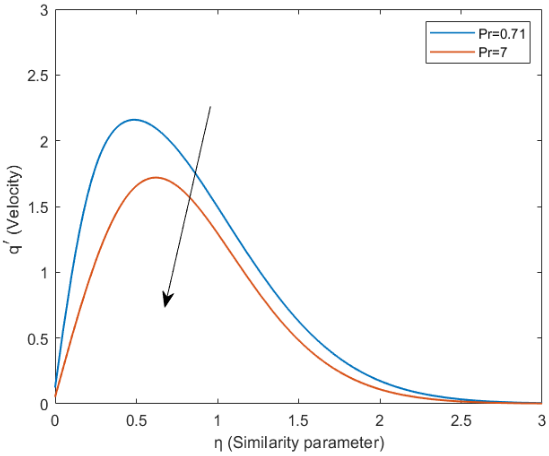

Fig. 12. Velocity profile for various values of and Gr=5, Gc=2, Pr=0.71, Sc=0.6, M=10, R=5, Q=1, γ=0.5, K=0.5, Df=0.2, h=1.5, t=0.1, Ω=0.5, w=30, k1=0.4

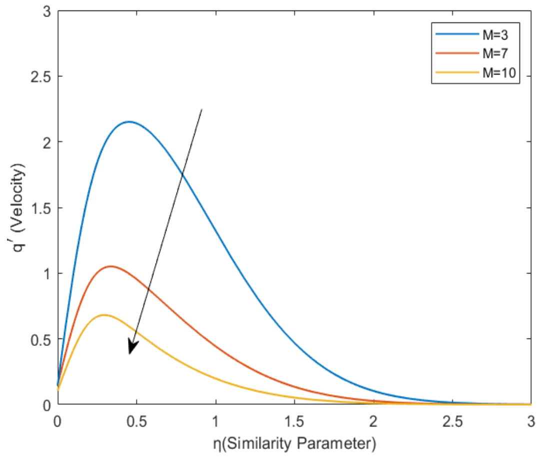

Fig. 13. Velocity profile for various values of M and Gr=5, Gc=2, Pr=7 Sc=0.6, M=10, R=5.0, Q=1.0, γ=0.5, K=0.5, Df=0.2, h=1.5, t=0.1, w=30, Ω=0.5, k1=0.4

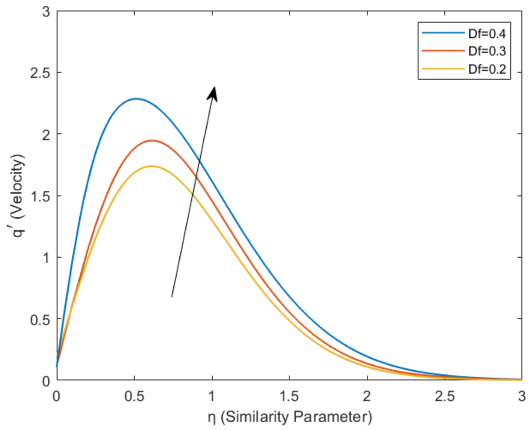

Fig. 14. Velocity Profile for various values of Df and =5, Gc=10, Pr=7, Sc=0.1 ,M=10, R=5, Q=1, $\gamma = 0.5$, K=0.5, Df=0.1, h=1.5, t=0.1 w=30, Ω =0.5, k1=0.4

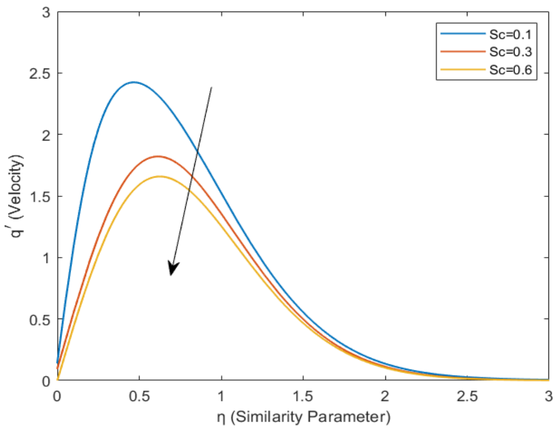

Fig. 15. Velocity for distinct values of S_c and Gr=5, Gc=10, Pr=7, M=10, R=5, Q=1, $\gamma = 0.5$, K=0.5, Df=0.1, h=1.5, t=0.1 w=30, Ω =0.5, k1=0.4

Figure 16 and Figure 17 shows the plate's velocity contours, where an increase in velocity is associated with a rise in the Grashof number (Gr). This suggests that buoyancy forces have a significant impact on enhancing the fluid's velocity near the plate and Figure 18 illustrates how the velocity of the plate decreases as the thermal radiation parameter (R) increases. This shows that increased thermal radiation reduces the fluid's velocity, potentially due to the reduction in heat transfer efficiency. Figure 19 demonstrates that the velocity also decreases as the chemical reaction parameter (K) increases. This highlights the suppressive effects of chemical reactions on fluid motion, likely due to changes in species concentration affecting the overall flow dynamics.

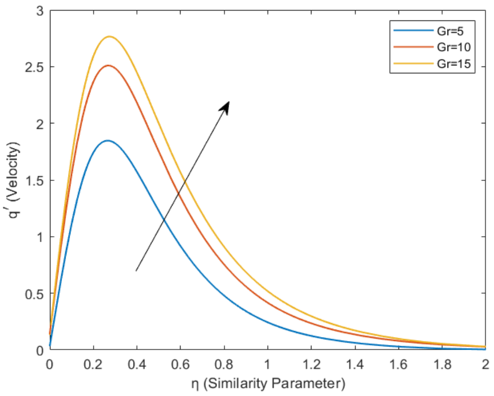

Fig. 16. Velocity profile for various values of Gr and Gc=10, Pr=7, Sc=0.1, M=10, R=5, Q=1, $\gamma = 0.5$, K=0.5, Df=0.1, h=1.5, t=0.1 w=30, Ω=0.5, k1=0.4

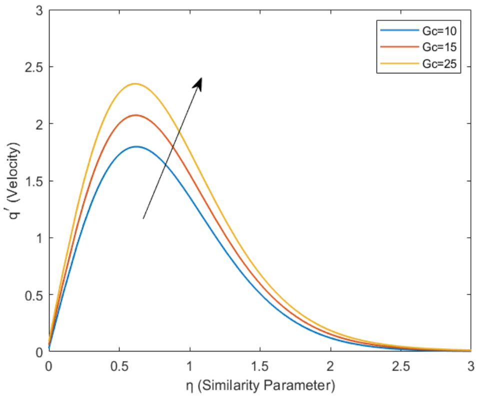

Fig. 17. Velocity profile for various values of Gc and Gr=10, Pr=7, Sc=0.1, M=10, R=5, Q=1,$\gamma = 0.5$, K=0.5, Df=0.1, h=1.5, t=0.1 w=30, Ω=0.5, k1=0.4

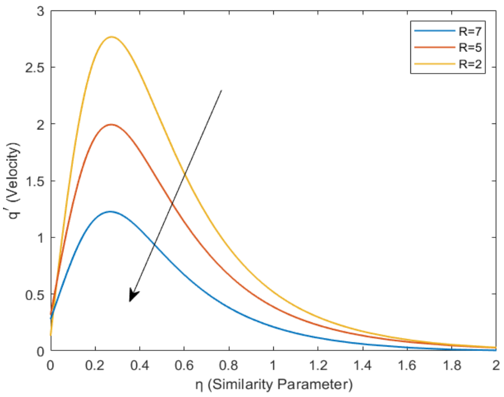

Fig. 18. Velocity profile for various values of R and Gc=10, Gr=10, Pr=7, Sc=0.1, M=10, R=5, Q=1, $\gamma = 0.5$, K=0.5, Df=0.1, h=1.5, t=0.1 w=30, Ω=0.5, k1=0.4

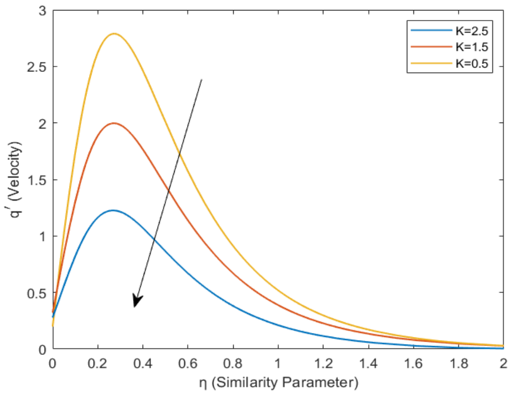

Fig. 19. Velocity profile for various values of K and Gc=10, Gr=10, Pr=7, Sc=0.1, M=10, R=5, Q=1, $\gamma = 0.5$, K=0.5, Df=0.1, h=1.5, t=0.1 w=30, Ω=0.5, k1=0.4

Figure 20 illustrate how the plate's velocity reaches peak performance as the Casson fluid parameter values increase, we can visualize this through a graph. A Casson fluid behaves more like a solid under low shear stress but flows like a fluid under higher shear stress.

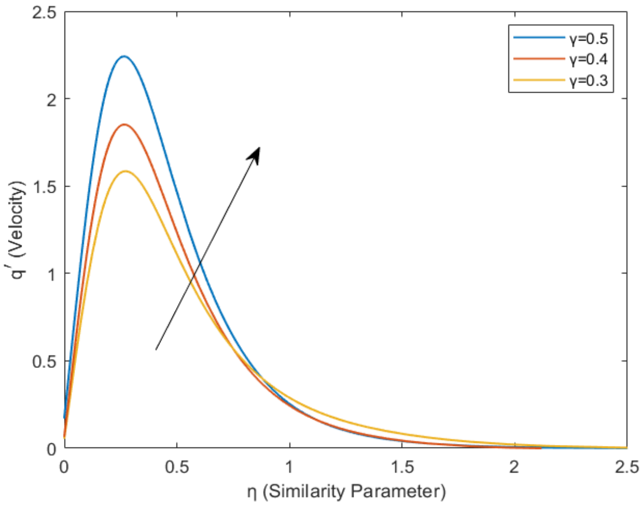

Fig. 20. Velocity graph for various values of γ and Gc=10, Gr=10, Pr=7, Sc=0.1, M=10, R=5, Q=1, K=0.5, Df=0.1, h=1.5, t=0.1 w=30, Ω=0.5, k1=0.4

Where $m^* = 2\left[\frac{M^2}{1+h^2} + i\left(\Omega - \frac{M^2 h}{1+h^2}\right)\right] + \frac{1}{k_1}$, a $= \left(\frac{Pr(R-Q)-ScK}{Pr-Sc}\right)$, $a_1 = 1 + \frac{1}{\gamma}$, $\eta = \frac{y}{2\sqrt{t}}$, $b = \frac{m^*+KSca_1}{a_1\, Sc-1}$, $c = \frac{a_1 Pr(R-Q)}{1-a_1 Pr}$, $d = \frac{Sc\, Ka_1 - m^*}{1-Sc\, a_1}$, erfc – Complementary error function

5. Conclusion

This research explores the interaction between rotational and Dufour effects on magnetohydrodynamic (MHD) Casson fluid flows, taking into account thermal radiation and chemical reactions at constant temperature and concentration. The study employs Laplace transforms to gain a deeper understanding of the governing equations and to interpret their fundamental behavior. Graphical representations are used to visualize and emphasize the findings. Here's a summary of the key results and trends observed

i. Effects on Temperature and Concentration Profiles:

As heat generation (Q) and time (t) increase, the temperature profile rises, contributing to a higher Dufour number (Df) also the Schmidt number (Sc) and Prandtl number (Pr) affect the concentration and temperature profiles, respectively and their increasing values may lead to a reversal in trends observed for these profiles.

The radiation parameter (R) and thermal conductivity (K) also interact with other parameters, influencing the temperature profile and potentially causing reversed trends depending on their magnitudes.

ii. Effects on Velocity Profiles:

An increase in magnetic parameter, thermal conductivity, Schmidt number, radiation parameter, and Prandtl number results in a decrease in fluid speed due to enhanced resistive forces or more stabilized fluids. Simultaneously, these changes can lead to a more significant Dufour effect and Caason fluid parameter reflecting increased importance of velocity profiles.

Overall ,the research highlights interactions among various parameters affecting the MHD Casson fluid flow. Increasing certain parameters can stabilize or resist fluid motion, leading to decreased speed and enhanced Dufour effects. Conversely, these changes can also lead to reversed trends in temperature and concentration profiles, demonstrating the intricate balance of forces in such fluid systems.

Acknowledgement
The authors are highly grateful to the reviewers for their valuable comments and suggestions on improving the quality of work. The authors are also grateful to the editors / publishers of all those journals and books from where the literature for this article has been reviewed and discussed.

References

[1] Soundalgekar, V. M., M. R. Patil, and M. D. Jahagirdar. "MHD Stokes problem for a vertical infinite plate with variable temperature." *Nuclear Engineering and Design* 64, no. 1 (1981): 39-42. https://doi.org/10.1016/0029-5493(81)90030-3
[2] Chamkha, Ali J., Harmindar S. Takhar, and V. M. Soundalgekar. "Radiation effects on free convection flow past a semi-infinite vertical plate with mass transfer." *Chemical Engineering Journal* 84, no. 3 (2001): 335-342. https://doi.org/10.1016/S1385-8947(00)00378-8
[3] Kataria, Hari R., and Harshad R. Patel. "Radiation and chemical reaction effects on MHD Casson fluid flow past an oscillating vertical plate embedded in porous medium." *Alexandria Engineering Journal* 55, no. 1 (2016): 583-595. https://doi.org/10.1016/j.aej.2016.01.019
[4] Vijayaragavan, R., M. Ramesh, and S. Karthikeyan. "Heat and mass transfer investigation on MHD Casson fluid flow past an inclined porous plate in the effects of Dufour and chemical reaction." *Journal of Xi'an University of Architecture and Technology* 13, no. 6 (2021): 860-873.
[5] Kavitha, S., Ayothi Selvaraj, Senthamilselvi Sathiamoorthy, and P. Rajesh. "A Parabolic Flow with MHD, the Dufour and Rotational Effects of Uniform Temperature and Mass Diffusion through an Accelerating Vertical Plate in the Presence of Chemical Reaction." *Journal of Advanced Research in Fluid Mechanics and Thermal Sciences* 110, no. 2 (2023): 192-205. https://doi.org/10.37934/arfmts.110.2.192205
[6] Selvaraj, A., S. Dilip Jose, R. Muthucumaraswamy, and S. Karthikeyan. "MHD-parabolic flow past an accelerated isothermal vertical plate with heat and mass diffusion in the presence of rotation." *Materials Today: Proceedings* 46 (2021): 3546-3549. https://doi.org/10.1016/j.matpr.2020.12.499
[7] Nandakumar, V., S. Senthamilselvi, and Ayothi Selvaraj. "Soret and MHD Effects of Parabolic Flow Past through an Accelerated Vertical Plate with Constant Heat and Mass Diffusion in the Presence of Rotation, Chemical Reaction and Thermal Radiation." *Journal of Advanced Research in Fluid Mechanics and Thermal Sciences* 112, no. 1 (2023): 125-138. https://doi.org/10.37934/arfmts.112.1.125138
[8] Selvaraj, A., and E. Jothi. "Heat source impact on MHD and radiation absorption fluid flow past an exponentially accelerated vertical plate with exponentially variable temperature and mass diffusion through a porous medium." *Materials Today: Proceedings* 46 (2021): 3490-3494. https://doi.org/10.1016/j.matpr.2020.11.919
[9] Lakshmikaanth, D., A. Selvaraj, P. Selvaraju, and S. Dilip Jose. "Hall and Heat Source Effects of Flow Past a Parabolic Accelerated Isothermal Vertical Plate in the Presence of Chemical Reaction and Radiation." *JP Journal of Heat and Mass Transfer* 34 (2023): 105-126. https://doi.org/10.17654/0973576323035
[10] Maran, D., A. Selvaraj, M. Usha, and S. Dilipjose. "First order chemical response impact of MHD flow past an infinite vertical plate with in the sight of exponentially with variable mass diffusion and thermal radiation." *Materials Today: Proceedings* 46 (2021): 3302-3307. https://doi.org/10.1016/j.matpr.2020.11.464
[11] Aruna, M., A. Selvaraj, and V. Rekha. "Hall and Magnetic Impacts on Stream Past a Parabolic Accelerated Vertical Plate with Varying Heat and Uniform Mass Diffusion in the Appearance of Thermal Radiation." In *International Conference on Advancement in Manufacturing Engineering*, pp. 323-336. Singapore: Springer Nature Singapore, 2022. https://doi.org/10.1007/978-981-99-1308-4_26
[12] Radha, Ganesan, Ayothi Selvaraj, Soundararajan Bhavani, and Periasamy Selvaraju. "Magneto Hydrodynamic Effects on Unsteady Free Convection Casson Fluid Flow Past on Parabolic Accelerated Vertical Plate with Thermal Diffusion." *Journal of Advanced Research in Fluid Mechanics and Thermal Sciences* 116, no. 1 (2024): 184-200. https://doi.org/10.37934/arfmts.116.1.184200
[13] Muthukumaraswamy, R., and P. Ganesan. "Unsteady flow past an impulsively started vertical plate with heat and mass transfer." *Heat and Mass Transfer* 34, no. 2 (1998): 187-193. https://doi.org/10.1007/s002310050248
[14] Muthucumaraswamy, R., M. Thamizhsudar, and J. Pandurangan. "Hall Effects on MHD Flow Past an Exponentially Accelerated Vertical Plate in the Presence of Rotation." *Annals of the Faculty of Engineering Hunedoara* 12, no. 3 (2014): 145. https://doi.org/10.1515/ijame-2015-0039

[15] Hetnarski, R. "On inverting the Laplace transforms connected with the error function." *Applicationes Mathematicae* 4, no. 7 (1964): 399-405. https://doi.org/10.4064/am-7-4-399-405

[16] Hetnarski, Richard B. "An algorithm for generating some inverse Laplace transforms of exponential form." *Zeitschrift für angewandte Mathematik und Physik ZAMP* 26 (1975): 249-253. https://doi.org/10.1007/BF01591514

[17] Sarma, Subhrajit, and Nazibuddin Ahmed. "Dufour effect on unsteady MHD flow past a vertical plate embedded in porous medium with ramped temperature." *Scientific Reports* 12, no. 1 (2022): 13343. https://doi.org/10.1038/s41598-022-15603-x

[18] Prakash, J., and A. Selvaraj. "Effects of Radiation and Heat Generation on MHD and Parabolic Motion on Casson Fluids Flow through a Rotating Porous Medium in a Vertical Plate." *Journal of Applied Mathematics & Informatics* 42, no. 3 (2024): 607-623.

[19] Reddy, B. Prabhakar, O. D. Makinde, and Alfred Hugo. "A computational study on diffusion-thermo and rotation effects on heat generated mixed convection flow of MHD Casson fluid past an oscillating porous plate." *International Communications in Heat and Mass Transfer* 138 (2022): 106389. https://doi.org/10.1016/j.icheatmasstransfer.2022.106389

[20] Reddy, N. Ananda, and K. Janardhan. "Soret and Dufour effects on MHD Casson fluid over a vertical plate in presence of chemical reaction and radiation." *International Journal of Current Research and Review* 9, no. 24 (2017): 55-61.

[21] Palani, G., and A. Arutchelvi. "MHD nanofluid flow past an inclined plate with soret and dufour effects." *JP Journal of Heat and Mass Transfer* 31 (2023): 123-145. https://doi.org/10.17654/0973576323009

[22] Kumar, M. A., and Y. D. Reddy. "Combined effects of chemical reaction, Dufour, Soret effects on unsteady MHD flow past an impulsively started inclined porous plate with variable temperature and mass diffusion." *International Journal of Mathematical Archive* 7, no. 9 (2016): 98-111.

[23] Vempati, S. R., and A. B. Laxmi-Narayana-Gari. "Soret and Dufour effects on unsteady MHD flow past an infinite vertical porous plate with thermal radiation." *Applied Mathematics and Mechanics* 31 (2010): 1481-1496. https://doi.org/10.1007/s10483-010-1378-9

[24] Muthucumaraswamy, R., and M. Radhakrishnan. "Chemical reaction effects on flow past an accelerated vertical plate with variable temperature and mass diffusion in the presence of magnetic field." *Journal of Mechanical Engineering and Sciences* 3 (2012): 251-260. https://doi.org/10.15282/jmes.3.2012.1.0023

[25] Muthucumaraswamy, R., N. Dhanasekar, and G. Easwara Prasad. "Mass transfer effects on accelerated vertical plate in a rotating fluid with first order chemical reaction." *Journal of Mechanical Engineering and Sciences* 3 (2012): 346-355. https://doi.org/10.15282/jmes.3.2012.11.0033

[26] Patel, Harshad R. "Effects of cross diffusion and heat generation on mixed convective MHD flow of Casson fluid through porous medium with non-linear thermal radiation." *Heliyon* 5, no. 4 (2019). https://doi.org/10.1016/j.heliyon.2019.e01555

[27] Dhanalakshmi, E., P. Rajesh, P. Kandan, M. Kesavan, G. Jayaraman, A. Selvaraj, and R. Priya. "Stability of bonds, kinetic stability, energy parameters, spectral characterization, GC-MS and molecular descriptors studies on coumarine, 3-[2-(1-methyl-2-imidazolylthio)-1-oxoethyl]." *Journal of Molecular Structure* 1295 (2024): 136544. https://doi.org/10.1016/j.molstruc.2023.136544

[28] Karthikeyan, S., A. Selvaraj, and M. Venkateswarlu. "Rotating significance of parabolical movement antique with an appearance on isothermal vertical plate by MHD." *Materials Today: Proceedings* 51 (2022): 1120-1123. https://doi.org/10.1016/j.matpr.2021.07.109

[29] Karthikeyan, S., and A. Selvaraj. "Uniform mass diffusion on thermal radiation with rotation of parabolic in progress vertical plate set MHD." *Materials Today: Proceedings* 51 (2022): 1074-1078. https://doi.org/10.1016/j.matpr.2021.07.098

[30] Gayathri, M., B. Hari Babu, and M. Veera Krishna. "Soret and Dofour effects on unsteady MHD convection flow over an infinite vertical porous plate." *Modern Physics Letters B* (2024): 2450449. https://doi.org/10.1142/S0217984924504499

[31] Kumar, Vasa Vijaya, M. N. Raja Shekar, and Shankar Goud Bejawada. "Role of Soret, Dufour Influence on Unsteady MHD Oscillatory Casson Fluid Flow an Inclined Vertical Porous Plate in the Existence of Chemical Reaction." *Journal of Advanced Research in Fluid Mechanics and Thermal Sciences* 110, no. 2 (2023): 157-175. https://doi.org/10.37934/arfmts.110.2.157175

[32] Kumar, Vasa Vijaya, Mamidi Narsimha Raja Shekar, and Shankar Goud Bejawada. "Heat and Mass Transfer Significance on MHD Flow over a Vertical Porous Plate in the Presence of Chemical Reaction and Heat Generation." *CFD Letters* 16, no. 5 (2024): 9-20. https://doi.org/10.37934/cfdl.16.5.920

[33] Lakshmikaanth, D., A. Selvaraj, and S. Bhavani. "Exploration of the Impacts of Hall Effect, Dufour Effect, and Heat Source on Parabolic Flow over an Infinite Vertical Plate in the Presence of Rotation, Chemical Reaction, and Radiation in a Porous Medium." *CFD Letters* 17, no. 1 (2025): 60-77. https://doi.org/10.37934/cfdl.17.1.6077

[34] Lakshmikaanth, D., A. Selvaraj, L. Tamilselvi, S. Dilip Jose, and V. Velukumar. "Hall and Heat Source Effects of Flow State on a Vertically Accelerating Plate in an Isothermal Environment, Including Chemical Reactions, Rotation, Radiation, and The Dufour Effect." *JP Journal of Heat and Mass Transfer* 37, no. 4 (2024): 491-520. https://doi.org/10.17654/0973576324034

[35] Rafique, Khadija, Zafar Mahmood, Bilal Ali, Umar Khan, Taseer Muhammad, Nidhal Becheikh, and Lioua Kolsi. "Entropy analysis of Hall effect with variable viscosity and slip conditions on rotating hybrid nanofluid flow over nonlinear radiative surface." *Materials Today Communications* 39 (2024): 109167. https://doi.org/10.1016/j.mtcomm.2024.109167

[36] Rafique, Khadija, Zafar Mahmood, Aisha M. Alqahtani, Awatif M. A. Elsiddieg, Umar Khan, Wejdan Deebani, and Meshal Shutaywi. "Impacts of thermal radiation with nanoparticle aggregation and variable viscosity on unsteady bidirectional rotating stagnation point flow of nanofluid." *Materials Today Communications* 36 (2023): 106735. https://doi.org/10.1016/j.mtcomm.2023.106735

[37] Adnan, Waseem Abbas, Aisha M. Alqahtani, Zafar Mahmood, Sid Ahmed Ould Beinane, and Muhammad Bilal. "Numerical heat featuring in radiative convective ternary nanofluid under induced magnetic field and heat generating source." *International Journal of Modern Physics B* (2024): 2550044. https://doi.org/10.1142/S0217979225500444

[38] Khan, Umar, Zafar Mahmood, Sayed M. Eldin, Basim M. Makhdoum, Bandar M. Fadhl, and Ahmed Alshehri. "Mathematical analysis of heat and mass transfer on unsteady stagnation point flow of Riga plate with binary chemical reaction and thermal radiation effects." *Heliyon* 9, no. 3 (2023). https://doi.org/10.1016/j.heliyon.2023.e14472

[39] Ganie, Abdul Hamid, Zafar Mahmood, Mashael M. AlBaidani, N. S. Alharthi, and Umar Khan. "Unsteady non-axisymmetric MHD Homann stagnation point flow of CNTs-suspended nanofluid over convective surface with radiation using Yamada-Ota model." *International Journal of Modern Physics B* 37, no. 27 (2023): 2350320. https://doi.org/10.1142/S0217979223503204